Ⅴ．研究成果の刊行物・別刷

Journal of Cellular Physiology

Neutrophil Differentiation From Human-Induced Pluripotent Stem Cells

TATSUYA MORISHIMA,[1] KEN-ICHIRO WATANABE,[1] AKIRA NIWA,[2] HISANORI FUJINO,[1] HIROSHI MATSUBARA,[1] SOUICHI ADACHI,[1] HIROFUMI SUEMORI,[3] TATSUTOSHI NAKAHATA,[2] AND TOSHIO HEIKE[1]*

[1]*Department of Pediatrics, Graduate School of Medicine, Kyoto University, Kyoto, Japan*

[2]*Department of Clinical Application, Center for iPS Cell Research and Application, Kyoto University, Kyoto, Japan*

[3]*Laboratory of Embryonic Stem Cell Research, Stem Cell Research Center, Institute for Frontier Medical Sciences, Kyoto University, Kyoto, Japan*

Induced pluripotent stem (iPS) cells are of potential value not only for regenerative medicine, but also for disease investigation. The present study describes the development of a neutrophil differentiation system from human iPS cells (hiPSCs) and the analysis of neutrophil function and differentiation. The culture system used consisted of the transfer of hiPSCs onto OP9 cells and their culture with vascular endothelial growth factor (VEGF). After 10 days, TRA 1-85^{+}CD34^{+}VEGF receptor-2 (VEGFR-2)^{high} cells were sorted and co-cultured with OP9 cells in the presence of hematopoietic cytokines for 30 days. Floating cells were collected and subjected to morphological and functional analysis. These hiPSC-derived neutrophils were similar to peripheral blood mature neutrophils in morphology, contained functional neutrophil specific granules, and were equipped with the basic functions such as phagocytosis, superoxide production, and chemotaxis. In the process of differentiation, myeloid cells appeared sequentially from immature myeloblasts to mature segmented neutrophils. Expression patterns of surface antigen, transcription factors, and granule proteins during differentiation were also similar to those of granulopoiesis in normal bone marrow. In conclusion, differentiation of mature neutrophils from hiPSCs was successfully induced in a similar process to normal granulopoiesis using an OP9 co-culture system. This system may be applied to elucidate the pathogenesis of various hematological diseases that affect neutrophils.

J. Cell. Physiol. 226: 1283–1291, 2011.

Neutrophils and/or myeloid differentiation are most commonly affected in various hematological diseases including inherited bone marrow failure syndromes and neutrophil function disorders. Responsible genes have been identified in most of these syndromes or diseases, but the association between the gene mutation and the specific phenotype is not always clear. Moreover, often patients who present with a specific syndrome lack mutations in the known genes (Alter, 2007). Understanding the pathophysiology of these syndromes has been challenging despite the information provided by recent molecular findings, and in many of these syndromes, experimental models have not yet been generated.

Murine models of human congenital and acquired diseases are invaluable for disease investigation, but they provide a limited representation of human pathophysiology because they often do not faithfully mimic human diseases. The differences between murine and human physiologies make human cell culture an essential complement to research with animal models of disease.

Induced pluripotent stem (iPS) cells are reprogrammed somatic cells with embryonic stem (ES) cell-like characteristics generated by the introduction of combinations of specific transcription factors (Takahashi and Yamanaka, 2006; Meissner et al., 2007; Okita et al., 2007; Takahashi et al., 2007; Yu et al., 2007; Park et al., 2008b). Given the robustness of the approach, direct reprogramming promises to be a facile source of patient-derived cell lines. Such lines would be immediately valuable not only for regenerative medicine, but for disease investigation and drug screening as well.

The pluripotency and self-renewal potential of ES cells contributes to their value in various fields of science (Evans and Kaufman, 1981). Previous studies using normal or gene-manipulated ES cells have helped elucidate the process of normal embryogenesis and the genetic mechanisms of certain diseases (Lensch and Daley, 2006; Tulpule et al., 2010). Use of human embryos, however, faces ethical controversies that hinder the applications of human ES cells (hESCs). In addition, it is difficult to generate patient- or disease-specific ES cells, which are required for their effective application. The use of iPS cells would avoid the controversies surrounding human embryonic stem cell research.

Patient-specific iPS cells can be used for the generation of disease-corrected, patient-specific cells for cell therapy applications. Disease-specific pluripotent cells capable of differentiation into the various tissues affected in each condition can also provide new insights into disease pathophysiology by permitting analysis in a human system, under controlled conditions in vitro. Recent studies reported the generation of disease-specific iPS cell lines from patients with a variety of diseases (Park et al., 2008a; Raya et al., 2009; Agarwal et al., 2010). Therefore, disease-specific iPS cells are expected to be good models for the investigation of different diseases, and

Contract grant sponsor: The Ministry of Education, Culture, Sports, Science and Technology, Japan.

*Correspondence to: Toshio Heike, Department of Pediatrics, Graduate School of Medicine, Kyoto University, 54 Kawahara-cho, Shogoin, Sakyo-ku, Kyoto 606-8507, Japan.
E-mail: heike@kuhp.kyoto-u.ac.jp

Received 21 May 2010; Accepted 20 September 2010

Published online in Wiley Online Library (wileyonlinelibrary.com), 13 October 2010.
DOI: 10.1002/jcp.22456

effective neutrophil differentiation systems are required to investigate the pathogenesis of various hematological conditions that affect neutrophils using human iPS cells (hiPSCs).

Recent reports describe in vitro culture systems for neutrophil differentiation from hESCs (Choi et al., 2009; Saeki et al., 2009; Yokoyama et al., 2009); however, neutrophil differentiation from hiPSCs has not yet been reported in detail. One of these studies demonstrated that myeloid differentiation could be induced from hiPSCs using the same methodology employed for their differentiation from hESCs (Choi et al., 2009), but the differentiation process and the functions of hiPSC-derived neutrophils were not shown in detail. A system for erythroid differentiation from primate ES and murine iPS cells by co-culture with OP9 stromal cells was developed in previous studies (Umeda et al., 2004; Umeda et al., 2006; Shinoda et al., 2007; Niwa et al., 2009). In the present study, a neutrophil differentiation system from hiPSCs was established by modifying the erythroid differentiation system, and the functions of the hiPSC-derived neutrophils and their differentiation process were analyzed in detail. This system may contribute to the elucidation of the pathogenesis of various blood diseases and the development of novel therapeutic approaches.

Materials and Methods

Maintenance of cells

The human iPS cell lines 201B6, 253G1 and 253G4 were a kind gift from Dr. Yamanaka (Kyoto University, Kyoto), and were generated from human dermal fibroblasts by retrovirus-mediated transfection of four (201B6) or three (253G1 and 253G4) transcription factors (Oct3/4, Sox2, and Klf4, with or without c-Myc) (Takahashi et al., 2007; Nakagawa et al., 2008). The human iPS cell lines and the human ES cell line KhES3-EGFPneo (KhES-3G) were maintained on mitomycin-C (Kyowa Hakko Kirin, Tokyo, Japan) -treated mouse embryonic fibroblasts (MEFs) in DMEM/F12 (Sigma-Aldrich, St. Louis, MO) supplemented with 20% Knockout™ Serum Replacement (Invitrogen, Carlsbad, CA), 5 ng/ml basic fibroblast growth factor (bFGF; R&D Systems, Minneapolis, MN), 1% non-essential amino acids solution (Invitrogen), 5 mM sodium hydroxide solution, 100 μM 2-mercaptethanol, and 2 mM L-glutamine. The culture medium was replaced daily with fresh medium. Colonies were passaged onto new MEFs every 3 or 4 days. The human ES cell line was used in conformity with The Guidelines for Derivation and Utilization of Human Embryonic Stem Cells of the Ministry of Education, Culture, Sports, Science, and Technology, Japan. OP9 stromal cells, which were a kind gift from Dr. Kodama (Osaka University, Osaka), were maintained in α-MEM (Invitrogen) supplemented with 20% fetal calf serum (FCS; Biological Industries, Bet Haemek, Israel).

Antibodies

The antibodies used for flow cytometric analysis included fluorescein isothiocyanate (FITC)-conjugated anti-human TRA 1-85 (R&D Systems), CD45 (Becton-Dickinson, Franklin Lakes, NJ) antibodies, phycoerythrin (PE)-conjugated anti-human CD11b, CD34 (Beckman Coulter, Fullerton, CA), CD13, CD16, CD33 (Becton-Dickinson) antibodies, and allophycocyanin (APC)-conjugated anti-human vascular endothelial growth factor receptor-2 (VEGFR-2) (eBioscience, San Diego, CA) antibody. The primary antibodies used for immunocytochemical analysis included goat anti-human lactoferrin (Santa Cruz Biotechnology, Santa Cruz, CA) and rabbit anti-human MMP9 (Abcam, Cambridge, UK). Biotinylated horse anti-goat or anti-rabbit antibodies (Vector Laboratories, Burlingame, CA) were used as secondary antibodies.

Differentiation of iPS cells

Methods used for the initial differentiation of iPS cells and cell sorting were based on earlier reports (Umeda et al., 2004, 2006). Briefly, trypsin-treated undifferentiated iPS cells were transferred onto OP9 cells and cultured with 20 ng/ml vascular endothelial growth factor (VEGF) (R&D Systems). After 10 days, the induced cells were harvested with cell dissociation buffer (Invitrogen), and sorted TRA 1-85^{+}CD34^{+}VEGFR-2^{high} cells were transferred onto fresh OP9 cells in six-well plates at a concentration of 3×10^3 cells per well. Sorted cells were cultured in α-MEM (Invitrogen) containing 10% FCS (Sigma, St Louis, MO), 50 μM 2-mercaptoethanol, 20 ng/ml interleukin (IL)-3, 100 ng/ml stem cell factor (SCF) (R&D Systems), and 10 ng/ml thrombopoietin (TPO) for 20 days. On day 20 after cell sorting, cytokines were changed into 20 ng/ml IL-3 and 10 ng/ml granulocyte colony-stimulating factor (G-CSF). IL-3, TPO and G-CSF were kindly provided by Kyowa Hakko Kirin.

Flow cytometric analysis and cell sorting

Cells were trypsinized and stained with antibodies. Dead cells were excluded by 4',6-diamidino-2-phenylindole (DAPI) staining. Samples were analyzed using an LSR flow cytometer and Cell Quest software (Becton Dickinson). Cell sorting was performed using a FACSVantage SE flow cytometer (Becton Dickinson).

Cytostaining

Floating cells were centrifuged onto glass slides using a Shandon Cytospin® 4 Cytocentrifuge (Thermo, Pittsburgh, PA), and analyzed by microscopy after May–Giemsa, myeloperoxidase (MPO), or alkaline-phosphatase staining. Sequential morphological analysis was performed as follows: all adherent cells including OP9 cells were trypsinized, harvested, and incubated in a new tissue-culture dish (Becton-Dickinson) for 1 h to eliminate adherent OP9 cells (Suwabe et al., 1998). Floating cells were then collected, centrifuged onto glass slides, and analyzed by microscopy after May–Giemsa staining. For immunocytochemical analysis, cells were fixed with 4% paraformaldehyde (PFA), immersed in citrate buffer, and autoclaved for 5 min at 121°C for antigen retrieval (Toda et al., 1999). The slides were then incubated with primary antibodies followed by application of the streptavidinbiotin complex immunoperoxidase technique with diaminobenzidine as chromogen, and nuclei were counterstained with hematoxylin.

Electron microscopy

Cells were fixed in 2% glutaraldehyde in 0.1 M phosphate buffer (PB) for at least 2 h, and then postfixed in 1% osmium tetroxide in 0.1 M PB for 1.5 h. After fixation, samples were dehydrated in a graded ethanol series, cleared with propylene oxide, and embedded in Epon. Thin sections of cured samples were stained with uranyl acetate and Reynolds lead citrate. The sections were inspected using a transmission electron microscope, H7650 (Hitachi, Tokyo, Japan).

Chemotaxis assay

Chemotactic ability was determined using a modified Boyden chamber method (Boyden, 1962; Harvath et al., 1980). Briefly, 500 μl of the reaction medium (Hank's Balanced Salt Solution (HBSS) containing 2.5% FCS) with or without 10 nM formyl-Met-Leu-Phe (fMLP; Sigma-Aldrich) was placed into each well of a 24-well plate, and the cell culture insert (3.0-μm pores; Becton Dickinson) was gently placed into each well to divide the well into upper and lower sections. Floating cells were suspended in the reaction medium at 7.0×10^4/ml, and a 500-μl cell suspension was added to the upper well, allowing the cells to migrate from the upper to the lower side of the membrane for 4 h at 37°C. After incubation, cells in the lower chamber were collected and counted using an LSR flow cytometer. Cells were counted by flow cytometry as follows:

equivalent amounts of counting beads were added to each sample and counted until the bead count reached 10,000.

MPO activity assay

The EnzChek Myeloperoxidase (MPO) Activity Assay Kit (Molecular Probes, Leiden, The Netherlands) was used for rapid and sensitive determination of MPO chlorination activity in cell lysates. The procedure was performed following the manufacturer's instructions. Cell lysate samples were prepared from 1×10^4 floating cells by freeze-thaw cycles. Fluorescence was measured with a fluorescence microplate reader (Wallac 1420 ARVO sx; PerkinElmer, Waltham, MA) using fluorescence excitation and emission at 485 and 530 nm, respectively. The background fluorescence measured for each zero-MPO control reaction was subtracted from each fluorescence measurement before plotting.

DHR assay

Neutrophil production of reactive oxygen species was detected by flow cytometry using dihydrorhodamine123 (DHR) as described previously (Vowells et al., 1995). Briefly, 3.5×10^4 floating cells were suspended in 100 μl of the reaction buffer (HBSS containing 0.1% FCS and 5 mM glucose) per tube, and two tubes were prepared for each sample. Catalase (Sigma-Aldrich) at a final concentration of 1000 U/ml and DHR at a final concentration of 1.0×10^5 nM were added and incubated for 5 min in a 37°C shaking water bath. After incubation, phorbol myristate acetate (PMA; Sigma-Aldrich) at a final concentration of 400 ng/ml was added to one of the two tubes and tubes were returned to the water bath for an additional 15 min. Following incubation, rhodamine fluorescence from the oxidized DHR was detected using an LSR flow cytometer.

Phagocytosis and detection of reactive oxygen species

Phagocytosis and neutrophil production of reactive oxygen species was detected by chemiluminescent microspheres (luminol-binding carboxyl hydrophilic microspheres; TORAY, Tokyo, Japan) as described previously (Uchida et al., 1985). Briefly, 2×10^4 floating cells were suspended in 50 μl of the reaction buffer (HBSS containing 20 mM N-2-hydroxyethylpiperazine-N′-2-ethanesulfonic acid (HEPES)) per tube. To activate the system, 5 μl of chemiluminescent microspheres was added, and light emission was recorded continuously. During the measurement, samples were kept at 37°C. To inhibit the phagocytosis, 1.75 μg of cytochalasin B (Sigma-Aldrich) was added to the sample. Chemiluminescence from the microspheres was detected using a luminometer (TD-20/20; Turner Designs, Sunnyvale, CA).

RNA extraction and RT-PCR analysis

RNA samples were prepared using silica gel membrane-based spin-columns (RNeasy Mini-Kit™, Qiagen, Valencia, CA) and subjected to reverse transcription (RT) with the Ominscript-RT Kit™ (Qiagen). All procedures were performed following the manufacturer's instructions. For reverse transcriptase-polymerase chain reaction (RT-PCR), yields were adjusted by dilution to produce equal amounts of the human glyceraldehyde-3-phosphate dehydrogenase (GAPDH) amplicon. The complementary DNA (cDNA) templates were initially denatured at 94°C for 5 min, followed by 30–40 amplification reactions consisting of 94°C for 15–30 sec (denaturing), 55–63°C for 15–30 sec (annealing), and 72°C for 30–60 sec (extension), with a final extension at 72°C for 7 min. The oligonucleotide primers were as follows: NANOG, 5′-CAG CCC TGA TTC TTC CAC CAG TCC C-3′ and 5′-TGG AAG GTT CCC AGT CGG GTT CAC C-3′ (Takahashi et al., 2007); human GAPDH, 5′-CAC CAG GGC TGC TTT TAA CTC TG-3′ and 5′-ATG GTT CAC ACC CAT GAC GAA C-3′ (Umeda et al., 2006); PU.1, 5′-CTG CAT TGG CCC CCA CCG AG-3′ and 5′-AGG TCT TCT GAT GGC TGA GGG GG-3′; C/EBPα, 5′-TAA CCT TGT GCC TTG GAA ATG CAA AC-3′ and 5′- ATG TTT CCA CCC CTT TCT AAG GAC A-3′ (Duan and Horwitz, 2003); C/EBPε, 5′- AGT CTG GGG AAG AGC AGC TTC-3′ and 5′- ACA GTG TGC CAC TTG GTA CTG-3′ (Mori et al., 2009); MPO, 5′-TGA GGA CGG CTT CTC TCT TC-3′ and 5′-CCC GGT AAG TGA TGA TCT GG-3′; Lactoferrin, 5′-AGC TGG CAG ACT TTG CGC T-3′ and 5′-TTC AGA TTA GTA ATG CCT GCG ACA TAC-3′ (Kholodnyuk et al., 2006); Gelatinase (MMP-9), 5′-GCC TCC AAC CAC CAC CAC AC-3′ and 5′-GCC CAG CCC ACC TCC ACT C-3′ (Sugimoto et al., 2001); mouse GAPDH, 5′-ACG GCC GCA TCT TCT TGT GCA-3′ and 5′-CAC CCT TCA AGT GGG CCC CG-3′. PCR amplification reaction cycles were performed in the linear range for each primer by carrying out primer titrations. The number of reaction cycles per sample were: NANOG, 35 cycles; human GAPDH, 30 cycles; PU.1, 40 cycles; C/EBPα, 40 cycles; C/EBPε, 40 cycles; MPO, 35 cycles; Lactoferrin, 35 cycles; Gelatinase (MMP-9), 40 cycles; mouse GAPDH, 30 cycles.

Statistics

Statistical analyses were conducted using the Student's *t*-test. Statistical significance was defined as $P < 0.05$.

Results

Neutrophil differentiation from hiPSCs in co-culture with OP9 stromal cells

A culture system for the induction of erythroid cell differentiation from primate ES and murine iPS cells by co-culture with OP9 stromal cells (Umeda et al., 2004; Umeda et al., 2006; Shinoda et al., 2007; Niwa et al., 2009) was established, and this system was applied for neutrophil differentiation from hiPSCs. Prior data in primate ES cells suggested that the VEGFR-2^{high} fraction of differentiated cells contained hemangioblasts and VEGFR-2^{high}CD34$^+$ cells had more hematopoietic potential (Umeda et al., 2006). Therefore, the expression of VEGFR-2 and CD34 was examined using three human iPS cell lines (201B6, 253G1, 253G4) and one ES cell line (KhES-3G). After 10 days of co-culture with OP9 in the presence of 20 ng/ml VEGF, VEGFR-2^{high}CD34$^+$ cells appeared from all hiPSC lines in a similar manner to the ES cell line (Fig. 1A). Among these three human iPS cell lines, the highest percentage of VEGFR-2^{high}CD34$^+$ cells was detected in 253G4 (Fig. 1B), and the data on this cell line is therefore presented below.

The VEGFR-2^{high}CD34$^+$ cell fraction was sorted (Fig. 1C) and 1.1×10^4 (range; 0.6–2.2×10^4 in 14 independent cultures) VEGFR-2^{high}CD34$^+$ cells were grown in one 10-cm dish containing hiPSCs. They were then transferred onto fresh OP9 cells and cultured in the presence of hematopoietic cytokines. Around 10 days after cell sorting (day10 + 10), small, round cell colonies appeared (Fig. 1D), and these colonies gradually grew in both size and number (Fig. 1E). At the same time, floating cells also appeared, and the average number of floating cells from 1×10^4 sorted VEGFR-2^{high}CD34$^+$ cells at 30 days after cell sorting (day10 + 30) was 4.1×10^4 (range; 0.2–9.9×10^4 in 11 independent cultures).

May–Giemsa staining of the floating cells on day 10 + 30 revealed that 38.0 ± 1.6% of the cells were stab and segmented neutrophils (Fig. 1F), which were positive for MPO (Fig. 1G) and neutrophil alkaline-phosphatase (Fig. 1H). The rest were mainly immature myeloid cells and a small number of macrophages, and cells of other lineages, such as erythroid or lymphoid cells, were not observed. The frequency of MPO- and neutrophil alkaline-phosphatase-positive cells is shown in Table 1. The results were consistent with the morphological features revealed by May–Giemsa staining.

Surface marker analysis revealed that these floating cells were positive for CD45 and CD11b, and partially positive for CD13, CD33, and CD16 (Fig. 1I). The expression pattern of these surface markers was similar to that of neutrophils or immature myeloid cells in healthy bone marrow (van Lochem et al., 2004), although the CD16 expression level was lower.

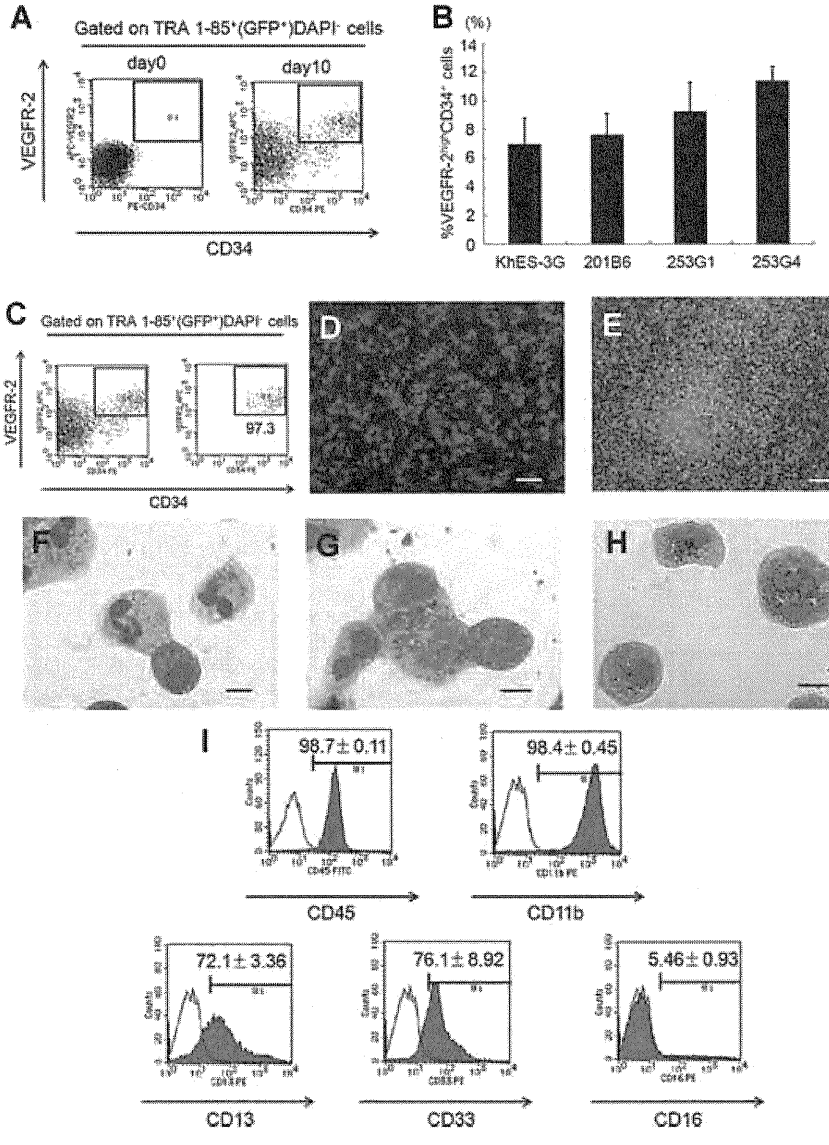

Fig. 1. Neutrophil differentiation from hiPSCs in co-culture with OP9 stromal cells. (A–B) Flow cytometric analysis of VEGFR-2 and CD34 during differentiation induction. TRA 1-85$^+$ (GFP$^+$) DAPI$^-$ cells were gated as human iPS (ES) cell-derived viable cells. Undifferentiated iPS (ES) cells and 10-day culture cells were stained with antibodies specific for VEGFR-2 and CD34. Representative results from one of three independent experiments (A) and percentages of VEGFR-2^{high}CD34$^+$ cells on day 10 (B) are shown (n = 3; bars represent SDs). (C) VEGFR-2^{high}CD34$^+$ cells were sorted on day 10. Representative dot plots and percentages of gated cells are shown. Purities of viable VEGFR-2^{high}CD34$^+$ cells were calculated at 95.5 ± 1.9% from 14 independent experiments. (D–E) Micrographs of adherent hematopoietic cell clusters generated on day 10 (D) and day 30 (E) after cell sorting. Scale bars: 200 μm. (F–H) May–Giemsa staining (F), myeloperoxidase staining (G), and neutrophil alkaline-phosphatase staining (H) of floating cells on day10 + 30. Scale bars: 10 μm. (I) Flow cytometric analysis of floating cells on day10 + 30 were stained with antibodies specific for CD45, CD11b, CD13, CD33, or CD16. Plots show the negative control profile (open bars) versus the specific antibody staining profiles (shaded bars). Representative results from one of three independent experiments are shown. [Color figure can be viewed in the online issue, which is available at wileyonlinelibrary.com.]

TABLE 1. Frequency of staining-positive cells for neutrophil specific granules

Staining	Frequency of positive cells (%)
Myeloperoxidase	93.7 ± 1.7
Neutrophil alkaline-phosphatase	39.0 ± 2.2
Lactoferrin	79.0 ± 1.4
Gelatinase	59.0 ± 3.7

Data are shown as mean ± SD (n = 3 independent experiments).

This lower CD16 expression level was similar to that of neutrophils derived in vitro from bone marrow CD34$^+$ cells by stimulation with G-CSF (Kerst et al., 1993b) and to the effect in vivo when G-CSF is administered to healthy volunteers (Kerst et al., 1993a). These results indicated that the modified OP9 co-culture system could differentiate mature neutrophils from immature hiPSCs.

hiPSC-derived neutrophils contain neutrophil specific granules

Mature neutrophils in vivo have intracellular granules that are important for their bactericidal function. The granules can be

classified into three types based on their size, morphology, or electron density, or with reference to a given protein: primary (azurophilic) granules contain MPO, secondary granules contain lactoferrin, and tertiary granules contain gelatinase (Borregaard and Cowland, 1997).

To assess the presence of these granules in hiPSC-derived neutrophils, they were imaged using transmission electron microscopy, which showed that the hiPSC-derived mature neutrophils contained peroxidase-positive and negative granules, as was observed in peripheral blood neutrophils (Fig. 2A–B). Immunocytochemical analysis revealed that hiPSC-derived mature neutrophils were also positive for lactoferrin and gelatinase (Fig. 2C–D). The frequencies of cells that were positive for neutrophil specific granules, as observed by transmission electron microscopy (Table 2) and immunocytochemical analysis (Table 1), were more than 90% for primary granules, about 80% for secondary granules, and approximately 60% for tertiary granules. These results indicated that hiPSC-derived neutrophils contained neutrophils-specific granules.

TABLE 2. Frequency of positive cells for neutrophil specific granules under transmission electron microscopy

Granules	Frequency of positive cells (%)
Peroxidase-positive granules	95.1 (135/142)
Peroxidase-negative granules	86.6 (123/142)

hiPSC-derived neutrophils exhibit biological bactericidal activities

Because neutrophils patrol circulating blood and play a key role in early phase defense mechanisms, the chemotactic, phagocytotic, and bactericidal activities of hiPSC-derived neutrophils were analyzed.

Chemotactic activity was assessed using a modified Boyden chamber method (Boyden, 1962; Harvath et al., 1980). After incubation with or without fMLP in the lower well, neutrophils had migrated from the upper side to the lower side of the membrane. Incubation with fMLP caused an increase in the number of migrated cells of more than three times compared to cells without fMLP, suggesting that hiPSC-derived neutrophils had chemotactic activity in response to a chemoattractant similar to natural neutrophils derived from bone marrow (Fig. 3A).

The MPO-dependent chlorination activity and reactive oxygen production of hiPSC-derived neutrophils, which are both essential for their bactericidal function, were determined next. MPO reacts with hydrogen peroxide (H_2O_2) to form the active redox and enzyme intermediate compound MPO-I, which oxidizes chloride (Cl^-) to HOCl (Winterbourn, 2002). As shown in Figure 3B, hiPSC-derived neutrophils showed MPO-dependent chlorination activity. To evaluate reactive oxygen production, the ability to convert DHR to rhodamine was assessed using flow cytometry (Vowells et al., 1995) and the results revealed that hiPSC-derived neutrophils characteristically produced superoxide in response to PMA (Fig. 3C).

Finally, phagocytotic activity and phagosome-dependent reactive oxygen production were measured using luminol-bound microspheres (Uchida et al., 1985). As shown in Figure 3D, the captured data confirmed that hiPSC-derived neutrophils could produce reactive oxygen species in response to the phagocytosis of microspheres, which was completely abolished in the presence of the antiphagocytic agent cytochalasin B. Moreover, transmission electron microscopy successfully captured a screenshot of a neutrophil phagocytosing the microbeads (Fig. 3E). The above results clearly show that neutrophils derived from hiPSC using the present culture system maintain their functional status.

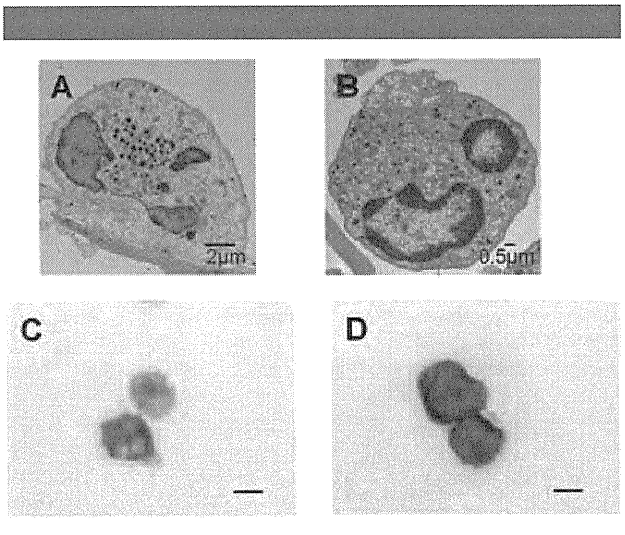

Fig. 2. Neutrophil-specific granules in hiPSC-derived neutrophils. (A–B) Floating cells on day10 + 30 (A) and peripheral blood neutrophils (B) were analyzed by transmission electron microscope. (C–D) Immunocytochemical analysis. Floating cells on day10 + 30 were stained for lactoferrin (C) and MMP9 (gelatinase) (D). Scale bars: 10 μm. [Color figure can be viewed in the online issue, which is available at wileyonlinelibrary.com.]

Step-wise neutrophil differentiation from hiPSCs is similar to normal granulopoiesis

Disorders of neutrophil differentiation are observed in various hematological diseases, among them the maturation arrest of neutrophil precursors in the bone marrow at the promyelocyte stage in severe congenital neutropenia. Thus, in clinical applications for disease investigation, the sequential analysis of the differentiation process from hiPSC to mature neutrophils in this culture system is required.

Observation of the sequential changes in cell morphology was done using May–Giemsa staining. Visualization of the morphology of day10 + 10 cells revealed that the cells were mainly myeloblasts and promyelocytes (Fig. 4A). On day10 + 20, myelocytes and metamyelocytes became predominant (Fig. 4B), and on day 10 + 30, stab and segmented neutrophils became predominant (Fig. 4C).

Surface antigen expression at each differentiation stage of hiPSC-derived cells was analyzed by flow cytometry (Fig. 4D). CD34, cell surface marker on normal immature hematopoietic cells, was detected in about 20% of the cells on day 10 + 10, but disappeared gradually thereafter. From day 10 + 10 to 10 + 30, the common myeloid antigens CD11b and CD33 were expressed in almost all the cells. Interestingly, expression of CD13, also a common myeloid antigen, was observed in less than 20% of cells at day 10 + 10 and did not subsequently increase. The expression level of CD16, which is a representative marker of matured neutrophils (van de Winkel and Anderson, 1991), doubled from day 10 + 10 to day 10 + 20, although the increase in expression was not statistically significant. These expression patterns were consistent with the patterns observed during normal neutrophil differentiation in healthy bone marrow (van Lochem et al., 2004).

The gene expression patterns of the pluripotency marker, transcription factors and granule proteins during neutrophil

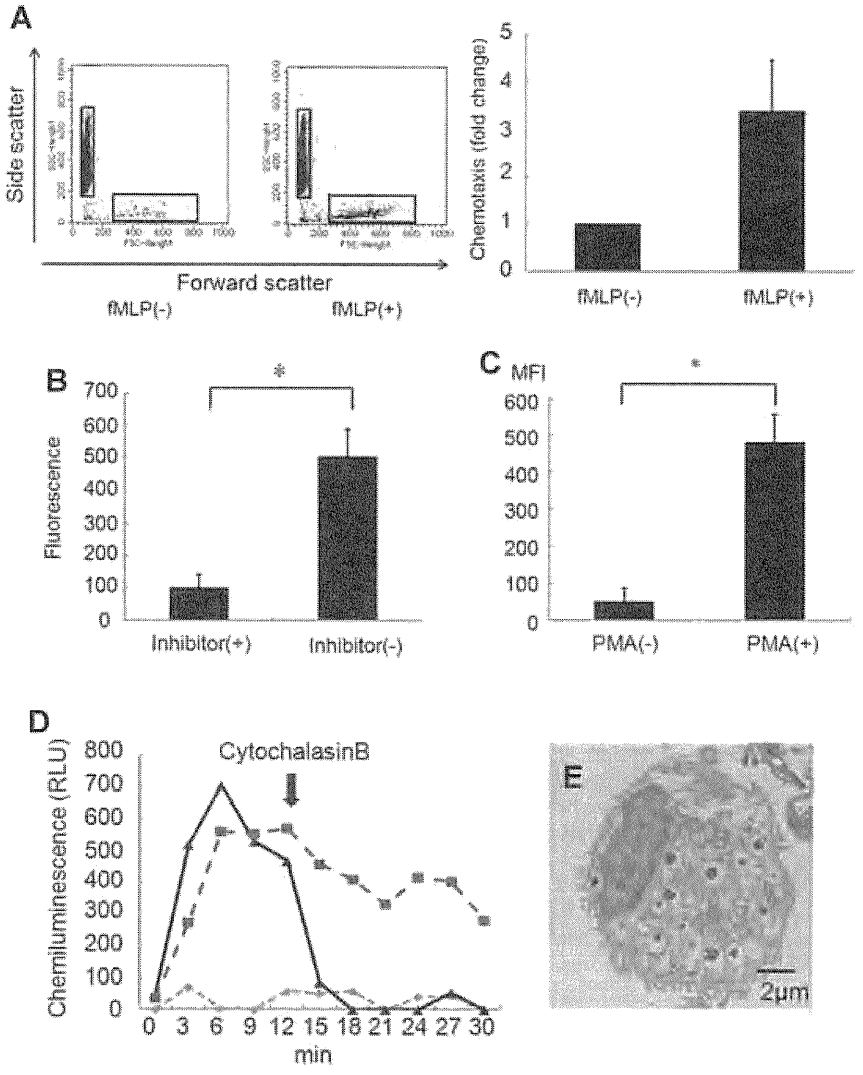

Fig. 3. Functional analysis of hiPSC-derived neutrophils. (A) Chemotactic activity of floating cells on day10 + 30 in response to fMLP was determined as described in Materials and Methods section. After a 4-h culture, the transwell inserts were removed, and the cells in the lower chamber were counted by an LSR flow cytometer (n = 3; bars represent SDs). (B) MPO chlorination activity in cell lysates from floating cells on day10 + 30 was analyzed by EnzChek Myeloperoxidase (MPO) Activity Assay Kit as described in the Materials and Methods section. The chlorination activity in neutrophil cell lysates was almost completely abolished by the addition of a chlorination inhibitor (n = 3; bars represent SDs; *P < 0.05.). (C) Floating cells on day10 + 30 were subjected to DHR assay. DHR was reacted with neutrophils with or without PMA, and the resultant rhodamine fluorescence was detected by flow cytometry. The addition of PMA increased the levels of fluorescence. Results are expressed as mean fluorescence intensity (MFI) (n = 3; bars represent SDs; *P < 0.05.). (D) Floating cells on day10 + 30 were subjected to the assay for phagocytosis-induced respiratory burst activity using chemiluminescent microspheres (luminol-binding microspheres). Gradual increase in chemiluminescence indicates the respiratory burst triggered by the phagocytosis of luminol-binding microspheres (squares). The increase in chemiluminescence was almost completely abolished by the addition of cytochalasin B (diamonds) and inhibited by its later addition (triangles). The figures are representative of three independent experiments. Abbreviation: RLU, relative light units. (E) hiPSC-derived neutrophils phagocytosing the microbeads were analyzed by transmission electron microscopy.

differentiation in this culture system were investigated by RT-PCR (Fig. 4E–F). NANOG, a pluripotency marker, was expressed in undifferentiated iPS cells but disappeared in sorted VEGFR2^{high}CD34^{+} cells after 10 days differentiation. PU.1 and C/EBPα, essential transcription factors for commitment and differentiation of the granulocytic lineage (Borregaard et al., 2001; Friedman, 2007) were first detected on day 10 + 10 and persisted thereafter. C/EBPε, which had a critical role for the later stages of neutrophil development and transcription of key granule proteins (Borregaard et al., 2001; Friedman, 2007) were first detected faintly on day 10 + 10 and upregulated thereafter. MPO and lactoferrin, which were expressed at the highest levels in myeloblasts/promyelocytes and myelocytes/metamyelocytes, respectively (Cowland and Borregaard, 1999; Borregaard et al., 2001), were detected on day 10 + 10. Gelatinase, which was expressed at the highest level in band and segmented neutrophilic cells (Cowland and Borregaard, 1999; Borregaard et al., 2001), was first detected on day 10 + 20 and upregulated thereafter. Altogether, these results suggested that the neutrophil differentiation in this co-culture system might recapitulate the orderly differentiation process in bone marrow.

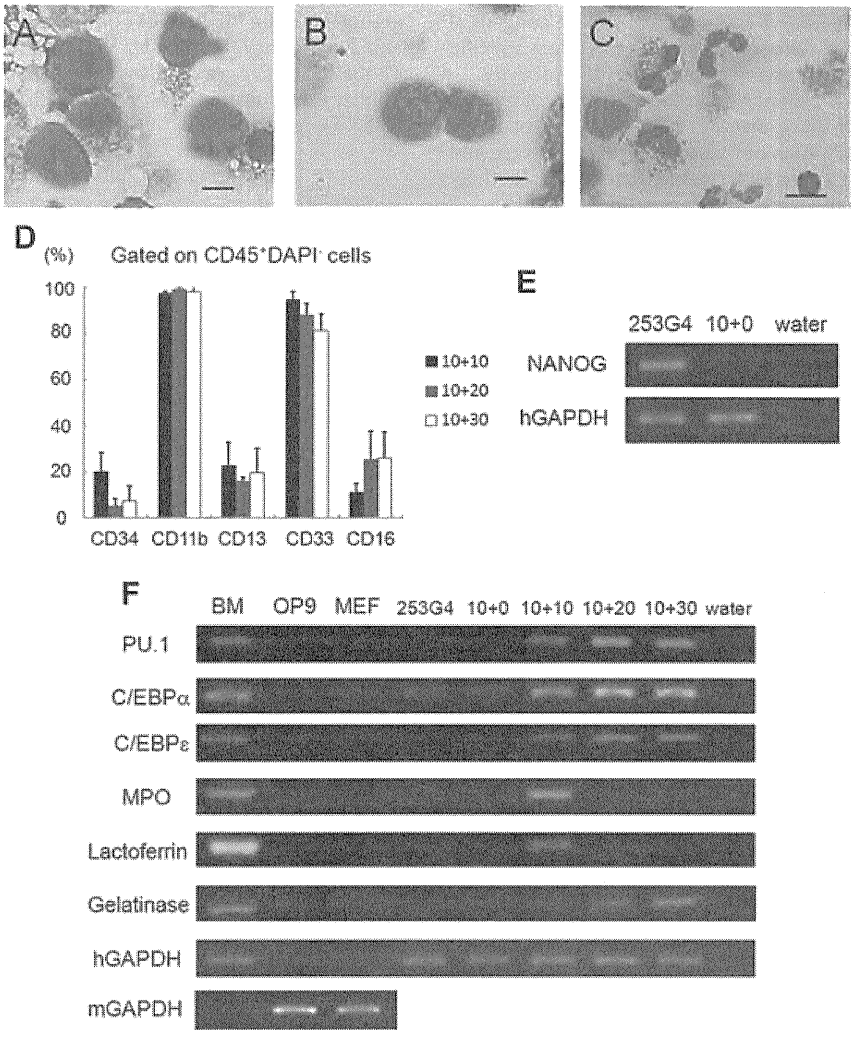

Fig. 4. Sequential analysis of neutrophil differentiation from hiPSCs. (A–C) Sequential morphological analysis of day 10 + 10 (A), day 10 + 20 (B) and day 10 + 30 (C). Scale bars: 10 μm. (D) Surface antigen expression at each level of differentiation of hiPSC-derived cells was analyzed by flow cytometry. All adherent cells including OP9 cells were harvested and stained with antibodies. Human $CD45^{+}DAPI^{-}$ cells were gated as hiPSC-derived viable leukocytes (n = 3; bars represent SDs). (E–F) Sequential RT-PCR analysis of a pluripotency marker (E), genes associated with neutrophil development and neutrophils-specific granules (F) during differentiation. Human GAPDH was used as a loading control. Abbreviations: BM, human bone marrow cells; 253G4, undifferentiated 253G4 cells; 10 + 0, sorted $VEGFR2^{high}CD34^{+}$ cells after 10 days differentiation; 10 + 10, 20, 30, all cells after 10, 20, 30 days differentiation after cell sorting; hGAPDH, human GAPDH; mGAPDH, mouse GAPDH. The figures are representative of three independent experiments. [Color figure can be viewed in the online issue, which is available at wileyonlinelibrary.com.]

Discussion

The analysis of the differentiation process of neutrophils can provide helpful information for the elucidation of the pathogenesis of hematopoietic diseases that affect neutrophils and/or myeloid differentiation, including inherited bone marrow failure syndromes and neutrophil function disorders. Traditionally, HL-60, an acute promyelocytic cell line, has been used as a neutrophil differentiation model (Collins et al., 1978; Newburger et al., 1979). Although this cell line grows well and differentiates easily into neutrophils, the neutrophil differentiation model is not suitable for the analysis of neutrophil-affected disorders because of its leukemic cell-origin. Development of a neutrophil differentiation system based on iPS cells would provide a better model for the analysis of such diseases, because iPS cells can be generated from the somatic cells of patients suffering from these diseases.

The current study aimed to investigate two issues in hiPSC-derived neutrophil differentiation: tracking the step-wise maturation in vitro and evaluating the wide spectrum of neutrophil functions. Through the use of a modified OP9 co-culture system, the directed and step-wise differentiation from hiPSCs to mature neutrophils containing neutrophil specific granules was first accomplished. The expression of surface antigens, transcription factors and granule proteins during differentiation exhibited the characteristic pattern of normal granulopoiesis. The biological functions of hiPSC-derived neutrophils were demonstrated through the quantitative assessment of granule enzyme activities and biological bactericidal activities such as chemotaxis and phagocytosis.

Defects in the maturation and function of neutrophils are associated with certain blood diseases including inherited bone marrow failure syndromes and neutrophil function disorders.

Among bone marrow failure syndromes, certain conditions affect a specific maturation stage, such as the maturation arrest at the plomyelocyte/myelocyte stage seen in severe congenital neutropenia. Neutrophil function disorders can affect specific bactericidal activities, such as the absence of MPO activity characteristic of MPO deficiency disorders. The use of hiPSCs for the investigation of these diseases requires sequential analyses that can identify each neutrophil maturation stage and include a functional analysis to evaluate each bactericidal activity separately on disease-specific, iPSC-derived neutrophils. Although previous studies have reported neutrophil differentiation models from hESCs (Choi et al., 2009; Saeki et al., 2009; Yokoyama et al., 2009) and hiPSC-derived neutrophils have been shown before (Choi et al., 2009), evidence showing that hiPSCs, which are artificially reprogrammed somatic cells, can follow the normal developmental pathway into fully functional mature neutrophils is of great significance, and the description of methods for identifying each neutrophil maturation step and analyzing each bactericidal pathway separately is important for clinical applications.

Although flow-cytometric analysis combined with RT-PCR identified the neutrophil maturation step relatively successfully, discrepancies between the neutrophil differentiation system in this study and normal granulopoiesis were noted such as the lower expression of CD16 than that shown by previous reports on hESC-derived neutrophils (Choi et al., 2009; Saeki et al., 2009; Yokoyama et al., 2009). As CD16 is a mature neutrophil marker in peripheral blood, two reasons could explain this phenomenon. First, residual precursors could have been more significant contaminants in the present system than in previously reported methods due to the function of cytokines and stroma supporting immature hematopoietic cells. Another possible reason is the shift of protein types between membrane-bound and soluble forms. Calluri previously reported that G-CSF is not only a myeloid cell growth factor, but also a modulator of neutrophil behavior (Carulli, 1997), and its stimulation decreases the membrane bound CD16 and increases its soluble form. Low CD16 expression has been documented in neutrophils derived in vitro from bone marrow $CD34^+$ cells by stimulation with G-CSF (Kerst et al., 1993b), and it has been observed in vivo when G-CSF is administered to healthy volunteers (Kerst et al., 1993a). This phenomenon, which is also documented in a report of hESC-derived neutrophils (Yokoyama et al., 2009), is unavoidable in differentiation culture systems using recombinant cytokines. The combination of flow cytometric and PCR analyses enables a more accurate staging of progenitors that could be of importance in the investigation of maturation arrest in future studies.

The culture system presented in this study is considered ineligible for clinical applications due to the use of xenogeneic factors such as OP9 cells and FCS. To overcome this problem, a xeno-free hematopoietic differentiation system from pluripotent cells is currently being established.

In conclusion, the present study shows the establishment of a fully functional mature neutrophil differentiation system from hiPSCs and the detailed analysis of their function and differentiation process. This system could become a useful tool for the investigation of various hematological diseases with defects in maturation and function of neutrophils.

Acknowledgments

We thank Dr. Yamanaka for providing the human iPS cell lines 201B6, 253G1, and 253G4, and Dr. Kodama for providing the OP9 cells. We are grateful to Kyowa Hakko Kirin for providing IL-3, TPO, and G-CSF. We also thank the Center for Anatomical Studies, Kyoto University Graduate School of Medicine for immunocytochemical analysis and transmission electron microscopy analysis. This work was supported by grants from the Ministry of Education, Culture, Sports, Science and Technology, Japan. This work was also supported by the Global COE Program "Center for Frontier Medicine" by the Ministry of Education, Culture, Sports, Science, and Technology (MEXT), Japan.

References

Agarwal S, Loh YH, McLoughlin EM, Huang J, Park IH, Miller JD, Huo H, Okuka M, Dos Reis RM, Loewer S, Ng HH, Keefe DL, Goldman FD, Klingelhutz AJ, Liu L, Daley GQ. 2010. Telomere elongation in induced pluripotent stem cells from dyskeratosis congenita patients. Nature 464:292–296.

Alter BP. 2007. Diagnosis, genetics, and management of inherited bone marrow failure syndromes. Hematology Am Soc Hematol Educ Program 29–39.

Borregaard N, Cowland JB. 1997. Granules of the human neutrophilic polymorphonuclear leukocyte. Blood 89:3503–3521.

Borregaard N, Theilgaard-Monch K, Sorensen OE, Cowland JB. 2001. Regulation of human neutrophil granule protein expression. Curr Opin Hematol 8:23–27.

Boyden S. 1962. The chemotactic effect of mixtures of antibody and antigen on polymorphonuclear leucocytes. J Exp Med 115:453–466.

Carulli G. 1997. Effects of recombinant human granulocyte colony-stimulating factor administration on neutrophil phenotype and functions. Haematologica 82:606–616.

Choi KD, Vodyanik MA, Slukvin II. 2009. Generation of mature human myelomonocytic cells through expansion and differentiation of pluripotent stem cell-derived lin-CD34+CD43+CD45+ progenitors. J Clin Invest 119:2818–2829.

Collins SJ, Ruscetti FW, Gallagher RE, Gallo RC. 1978. Terminal differentiation of human promyelocytic leukemia cells induced by dimethyl sulfoxide and other polar compounds. Proc Natl Acad Sci USA 75:2458–2462.

Cowland JB, Borregaard N. 1999. The individual regulation of granule protein mRNA levels during neutrophil maturation explains the heterogeneity of neutrophil granules. J Leukoc Biol 66:989–995.

Duan Z, Horwitz M. 2003. Targets of the transcriptional repressor oncoprotein Gfi-1. Proc Natl Acad Sci USA 100:5932–5937.

Evans MJ, Kaufman MH. 1981. Establishment in culture of pluripotential cells from mouse embryos. Nature 292:154–156.

Friedman AD. 2007. Transcriptional control of granulocyte and monocyte development. Oncogene 26:6816–6828.

Harvath L, Falk W, Leonard EJ. 1980. Rapid quantitation of neutrophil chemotaxis: use of a polyvinylpyrrolidone-free polycarbonate membrane in a multiwell assembly. J Immunol Methods 37:39–45.

Kerst JM, de Haas M, van der Schoot CE, Slaper-Cortenbach IC, Kleijer M, von dem Borne AE, van Oers RH. 1993a. Recombinant granulocyte colony-stimulating factor administration to healthy volunteers: induction of immunophenotypically and functionally altered neutrophils via an effect on myeloid progenitor cells. Blood 82:3265–3272.

Kerst JM, van de Winkel JG, Evans AH, de Haas M, Slaper-Cortenbach IC, de Wit TP, von dem Borne AE, van der Schoot CE, van Oers RH. 1993b. Granulocyte colony-stimulating factor induces hFc gamma RI (CD64 antigen)-positive neutrophils via an effect on myeloid precursor cells. Blood 81:1457–1464.

Kholodnyuk ID, Kozireva S, Kost-Alimova M, Kashuba V, Klein G, Imreh S. 2006. Down regulation of 3p genes, LTF, SLC38A3 and DRR1, upon growth of human chromosome 3-mouse fibrosarcoma hybrids in severe combined immunodeficiency mice. Int J Cancer 119:99–107.

Lensch MW, Daley GQ. 2006. Scientific and clinical opportunities for modeling blood disorders with embryonic stem cells. Blood 107:2605–2612.

Meissner A, Wernig M, Jaenisch R. 2007. Direct reprogramming of genetically unmodified fibroblasts into pluripotent stem cells. Nat Biotechnol 25:1177–1181.

Mori Y, Iwasaki H, Kohno K, Yoshimoto G, Kikushige Y, Okeda A, Uike N, Niiro H, Takenaka K, Nagafuji K, Miyamoto T, Harada M, Takatsu K, Akashi K. 2009. Identification of the human eosinophil lineage-committed progenitor: revision of phenotypic definition of the human common myeloid progenitor. J Exp Med 206:183–193.

Nakagawa M, Koyanagi M, Tanabe K, Takahashi K, Ichisaka T, Aoi T, Okita K, Mochiduki Y, Takizawa N, Yamanaka S. 2008. Generation of induced pluripotent stem cells without Myc from mouse and human fibroblasts. Nat Biotechnol 26:101–106.

Newburger PE, Chovaniec ME, Greenberger JS, Cohen HJ. 1979. Functional changes in human leukemic cell line HL-60. A model for myeloid differentiation. J Cell Biol 82:315–322.

Niwa A, Umeda K, Chang H, Saito M, Okita K, Takahashi K, Nakagawa M, Yamanaka S, Nakahata T, Heike T. 2009. Orderly hematopoietic development of induced pluripotent stem cells via Flk-1(+) hemoangiogenic progenitors. J Cell Physiol 221:367–377.

Okita K, Ichisaka T, Yamanaka S. 2007. Generation of germline-competent induced pluripotent stem cells. Nature 448:313–317.

Park IH, Arora N, Huo H, Maherali N, Ahfeldt T, Shimamura A, Lensch MW, Cowan C, Hochedlinger K, Daley GQ. 2008a. Disease-specific induced pluripotent stem cells. Cell 134:877–886.

Park IH, Zhao R, West JA, Yabuuchi A, Huo H, Ince TA, Lerou PH, Lensch MW, Daley GQ. 2008b. Reprogramming of human somatic cells to pluripotency with defined factors. Nature 451:141–146.

Raya A, Rodriguez-Piza I, Guenechea G, Vassena R, Navarro S, Barrero MJ, Consiglio A, Castella M, Rio P, Sleep E, Gonzalez F, Tiscornia G, Garreta E, Aasen T, Veiga A, Verma IM, Surralles J, Bueren J, Izpisua Belmonte JC., 2009. Disease-corrected haematopoietic progenitors from Fanconi anaemia induced pluripotent stem cells. Nature 460:53–59.

Saeki K, Nakahara M, Matsuyama S, Nakamura N, Yogiashi Y, Yoneda A, Koyanagi M, Kondo Y, Yuo A. 2009. A feeder-free and efficient production of functional neutrophils from human embryonic stem cells. Stem Cells 27:59–67.

Shinoda G, Umeda K, Heike T, Arai M, Niwa A, Ma F, Suemori H, Luo HY, Chui DH, Torii R, Shibuya M, Nakatsuji N, Nakahata T. 2007. alpha4-Integrin(+) endothelium derived from primate embryonic stem cells generates primitive and definitive hematopoietic cells. Blood 109:2406–2415.

Sugimoto C, Fujieda S, Sunaga H, Noda I, Tanaka N, Kimura Y, Saito H, Matsukawa S. 2001. Granulocyte colony-stimulating factor (G-CSF)-mediated signaling regulates type IV collagenase activity in head and neck cancer cells. Int J Cancer 93:42–46.

Suwabe N, Takahashi S, Nakano T, Yamamoto M. 1998. GATA-1 regulates growth and differentiation of definitive erythroid lineage cells during in vitro ES cell differentiation. Blood 92:4108–4118.

Takahashi K, Tanabe K, Ohnuki M, Narita M, Ichisaka T, Tomoda K, Yamanaka S. 2007. Induction of pluripotent stem cells from adult human fibroblasts by defined factors. Cell 131:861–872.

Takahashi K, Yamanaka S. 2006. Induction of pluripotent stem cells from mouse embryonic and adult fibroblast cultures by defined factors. Cell 126:663–676.

Toda Y, Kono K, Abiru H, Kokuryo K, Endo M, Yaegashi H, Fukumoto M. 1999. Application of tyramide signal amplification system to immunohistochemistry: a potent method to localize antigens that are not detectable by ordinary method. Pathol Int 49:479–483.

Tulpule A, Lensch MW, Miller JD, Austin K, D'Andrea A, Schlaeger TM, Shimamura A, Daley GQ. 2010. Knockdown of Fanconi anemia genes in human embryonic stem cells reveals early developmental defects in the hematopoietic lineage. Blood 115:3453–3462.

Uchida T, Kanno T, Hosaka S. 1985. Direct measurement of phagosomal reactive oxygen by luminol-binding microspheres. J Immunol Methods 77:55–61.

Umeda K, Heike T, Yoshimoto M, Shinoda G, Shiota M, Suemori H, Luo HY, Chui DH, Torii R, Shibuya M, Nakatsuji N, Nakahata T. 2006. Identification and characterization of hemoangiogenic progenitors during cynomolgus monkey embryonic stem cell differentiation. Stem Cells 24:1348–1358.

Umeda K, Heike T, Yoshimoto M, Shiota M, Suemori H, Luo HY, Chui DH, Torii R, Shibuya M, Nakatsuji N, Nakahata T. 2004. Development of primitive and definitive hematopoiesis from nonhuman primate embryonic stem cells in vitro. Development 131:1869–1879.

van de Winkel JG, Anderson CL. 1991. Biology of human immunoglobulin G Fc receptors. J Leukoc Biol 49:511–524.

van Lochem EG, van der Velden VH, Wind HK, te Marvelde JG, Westerdaal NA, van Dongen JJ. 2004. Immunophenotypic differentiation patterns of normal hematopoiesis in human bone marrow: reference patterns for age-related changes and disease-induced shifts. Cytometry B Clin Cytom 60:1–13.

Vowells SJ, Sekhsaria S, Malech HL, Shalit M, Fleisher TA. 1995. Flow cytometric analysis of the granulocyte respiratory burst: a comparison study of fluorescent probes. J Immunol Methods 178:89–97.

Winterbourn CC. 2002. Biological reactivity and biomarkers of the neutrophil oxidant, hypochlorous acid. Toxicology 181-182:223–227.

Yokoyama Y, Suzuki T, Sakata-Yanagimoto M, Kumano K, Higashi K, Takato T, Kurokawa M, Ogawa S, Chiba S. 2009. Derivation of functional mature neutrophils from human embryonic stem cells. Blood 113:6584–6592.

Yu J, Vodyanik MA, Smuga-Otto K, Antosiewicz-Bourget J, Frane JL, Tian S, Nie J, Jonsdottir GA, Ruotti V, Stewart R, Slukvin II, Thomson JA. 2007. Induced pluripotent stem cell lines derived from human somatic cells. Science 318:1917–1920 .

Review Article

Autoinflammatory diseases - a new entity of inflammation

Toshio Heike[1,*], Megumu K Saito[2], Ryuta Nishikomori[1], Takahiro Yasumi[1] and Tatsutoshi Nakahata[2]

[1]Department of Pediatrics, Graduate School of Medicine, Kyoto University, Kyoto, Japan
[2]Clinical Application Department, Center for iPS cell research and application, Kyoto University, Kyoto, Japan

The autoinflammatory diseases are characterized by seemingly unprovoked episodes of inflammation, without high-titer autoantibodies or antigen-specific T cells. The concept was proposed ten years ago with the identification of the genes underlying hereditary periodic fever syndromes. NLRP3 inflammasome activation and IL-1β secretion have recently emerged as a central mechanism in the pathogenesis of disease. Here we describe four genetically defined syndromes like cryopyrin-associated periodic syndromes (CAPS, cryopyrinopathies), mevalonate kinase deficiency (MKD) or hyper-IgD and periodic fever syndrome (HIDS), pyogenic aseptic arthritis, pyoderma gangrenosum, and acne syndrome (PAPA syndrome), and deficiency of interleukin-1-receptor antagonist (DIRA) along with the pitfall for understanding the pathphysiology.

Rec./Acc.2/7/2011

*Correspondence should be addressed to:
Toshio Heike

Key words:
autoinflammatory disease, NLRP3 inflammasome, IL-1β, cryopyrin-associated periodic fever (CAPS), mosaicism

Introduction

Inflammation has evolved as a physiologic mechanism necessary to defend our bodies from external and internal danger triggers such as infectious agents, chemical factors, and physical factors [1].

The innate immune system is assigned to recognize and encounter these stimuli. Recently, nucleotide-binding oligomerization domain (NOD)-like receptors (NLRs) have emerged as key players for the proper accomplishment of this process through recognition of pathogen associated molecular patterns (PAMPs) [2]. In addition to PAMPs, NLRs also sense endogenous stress signals known as damage associated molecular patterns (DAMPs) [2,3]. NLR dependent recognition of either exogenous or endogenous danger signals

initiates the recruitment of adaptor proteins and the formation of molecular platforms referred to as inflammasomes[2, 3]. In other word, inflammasomes are cellular alarts that assemble in response to microbial invasion and/or cellular damage and alert the system by triggering an inflammatory response. The subsequent activation of caspase-1 results in the post-transcriptional, proteolytic modulation of the related cytokines interleukin-1β (IL-1β) and IL-18 from their precursor to their active and secreted form, enhancing the inflammatory process. Among severalNLRs that form inflammasome platforms, the most studied are NALP1,NALP3 (NLRP3) and IPAF [2, 3, 4].

The identification of the critical role of NLRP3 inflammasome in the maturation of these inflammatory cytokines prompted the study of its role in the pathogenesis of several syndromes. The term IL-1β dependent autoinflammatory syndromes has been adopted for such syndromes. This group of diseases is characterized by defective regulation of innate immune response and the absence of autoantibodies or antigen-specific T cells [5].

Dysregulation of NLRP3 inflammasome based on mutations of inflammasome related genes has been implicated in the pathogenesis of cryopyrin-associated periodic fever syndrome (CAPS), hyper-IgD syndrome (HIDS), pyogenic arthritis, pyoderma gangrrenosum, and acne syndrome (PAPA), or deficiency of IL-1 receptor antagonist (DIRA) [6]. Interestingly, NLRP3 inflammasome activation by danger signals such as monosodium urate (MSU), calcium pyrophosphate dehydrate (CPPD), amyloid-beta, glucose or silica and asbestos is proposed as a key molecular mechanism in diseases including gout, pseudogout, Altheimer's disease, pulmonary fibrosis or the 2 diabetes mellitus [5].

We discuss in this review about this new-coming entity of diseases along with the pitfall for understanding the pathphysiology.

NLRP3 inflammasome

Recognition of microorganisms by the innate immune system depends on conserved germ line-encoded receptors called pattern-recognition receptors (PRRs) that sense conserved motifs present on microbes named PAMPs [7].

PRRs are classified into three groups: secreted, trans-membrane and cytosolic (Fig. 1). Secreted PRRs such as collectins, ficolins and pentraxins bind microbes and activate the complement system. The trans-membrane PRRs are Toll-like receptors (TLRs) and the C-type lectins, with some members expressed on cell surface (such as TLR2/4 and Dectin1/2) and some expressed on endosome membrane (TLR3/7/9). The cytosolic PRRs include the RIG-I-like receptors (RLRs), the nucleotide-binding domain leucine-rich repeat containing receptors (NLRs) and the newly identified DNA sensors AIM2 (absent in melanoma 2) and IFI16 (interferon-inducible protein16) [8,9,10]. Although the RLRs mainly detect viral pathogens, the NLRs can detect both PAMPs and DAMPs [11]. In response to PAMPs or DAMPs, a subset of NLRs forms a complex with ASC (apoptosis-associated speck-like protein containing a CARD) to activate caspase-1 [12]. In 2002, Tschopp group first named this complex the inflammasome [13]. Up to date, at least 4 different inflammasomes have been identified; they are the NLRP1, NLRP3, IPAF (NLRC4) and AIM2 inflammasomes [14].

NLRP3, also called CIAS1, PYPAF1, Cryopyrin, CLR1.1 (CATERPILLAR 1.1) or NALP3, is one of the best characterized NLR family members. In mice, NLRP3 is mainly expressed in tissues such as lung, liver, kidney, colon and ovary, with particularly high expression in the skin and eye [15, 16]. Mouse neutrophils, peripheral blood mononuclear cells (PBMCs) and bone marrow-derived dendritic cells (BMDCs) express high level of NLRP3 constitutively, while the bone marrow- derived macrophages (BMDMs) and Th2 cells only express this molecule at moderate level [15, 16]. However, upon TLR or TNF receptor stimulation, the expression of NLRP3 in BMDMs is dramatically elevated, largely as a result of NF-κB

activation [16, 17]. Both mouse and human osteoblasts express NLRP3 [18]. In addition, primary human PBMCs, the monocyte-derived THP-1 cell line, primary human keratinocytes (PK), keratinocyte-derived HaCaT cells, primary mast cells (MS), granulocytes and B cells all express NLRP3 [19, 20, 21]. The tissue distribution of human NLRP3 is also found in the urothelial layer in the bladder and in epithelial cells lining the oral and genital tracts besides the skin cells mentioned above [20,21].

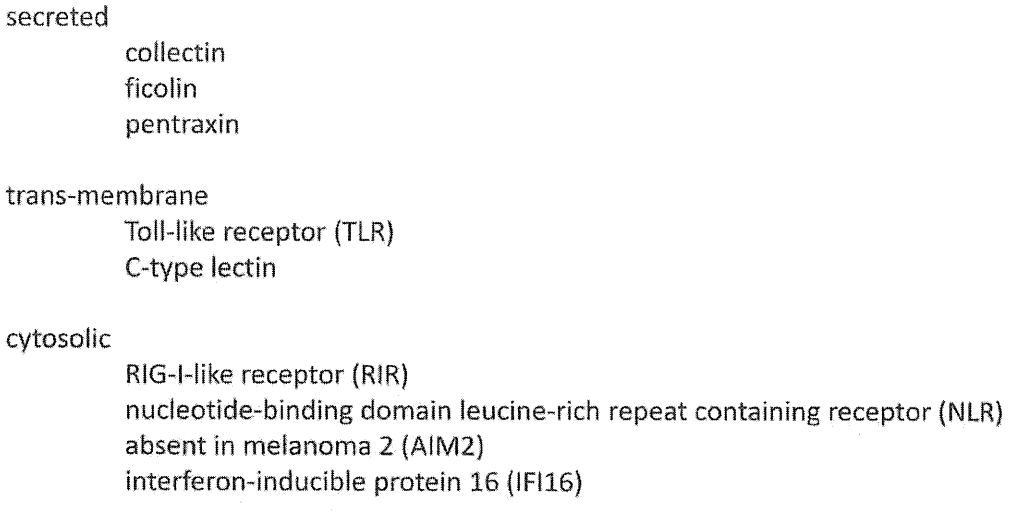

Fig. 1 Classification of pattern-recognition receptors

Recognition of microorganisms by the innate immune system depends on conserved germ line-encoded receptors called pattern-recognition receptors (PRRs) that sense conserved motifs present on microbes named PAMPs.
PRRs are classified into three groups: secreted, trans-membrane and cytosolic.

Structural analysis revealed that NLRP3 contains an N-terminal pyrin domain, an intermediate NACHT domain and a C-terminal LRR domain. Upon activation,NLRP3 recruits ASC via a pyrin-pyrindomain interaction and the recruited ASC binds to pro-caspase-1 via a CARD–CARD interaction. The multiprotein complex thus formed, now called the NLRP3 inflammasome, then activates caspase-1, and the latter cleaves pro-interleukin-1β (IL-1β) and pro-IL-18 to form mature IL-1β and IL-18, respectively (Fig. 2) [22]. Whole pathogens, PAMPs, DAMPs and environmental irritants can all activate the NLRP3 inflammasome. However, the exact mechanism(s) leading to NLRP3 inflammasome activation is still not clear. Given the diversity of these NLRP3 activators, a consensus is emerging that there is a common downstream intracellular activator that constitutes a final common pathway for NLRP3 activation (Fig. 2) [23,24]. In any case, the mature IL-1β and IL-18 production resulted from NLRP3 activation are highly potent proinflammatory mediators important for host defense against infectious agents. In addition, via IL-1β, the NLRP3 inflammasome is linked to Th17 cell differentiation [25,26] as well as to Th2 response since vaccination with aluminum adjutants also activates this inflammasome [27,28]. It should be noted, however, that NLRP3-mediated secretion of IL-1β and IL-18 must be under tight control, as excessive production of these cytokines can lead to autoinflammatory diseases. This is seen in the group of diseases collectively called cryopyrin(CIAS1, NLRP3)-associated periodic syndromes (CAPSs) which are caused by hyper-activation of the NLRP3 inflammasome due to mutations in the NLRP3 gene [29,30]. Besides, hyperimmunoglobulinemia D with periodic fever syndrome (HIDS), the deficiency of the IL-1 receptor antagonist (DIRA), and the syndrome of pyogenic arthritis with pyoderma gangrenosum and acne (PAPA) are caused by mutations in genes encoding proteins that directly or

indirectly correlate NLRP3 [8].

Cryopyrin-associated periodic syndrome (CAPS) or cryopyrinopathies

The cryopyrin-associated periodic syndrome spectrum, which encompass FCAS(Familial cold autoinflammatory syndrome), MWS(Muckle-Wells syndrome), and NOMID/CINCA syndrome (Neonatal onset multisystem inflammatory disease/chronic infantile neurologic, cutaneous, and articular syndrome), is caused by mutations in the cold induced autoinflammatory syndrome 1 (CIAS1) gene, first identified in 2001 [31]. CIAS1 codes for the protein cryopyrin, also known as NLRP3 or PYPAF1 [32]. We use the term NLRP3 thereafter. The cryopyrinopathies are transmitted in an autosomal dominant pattern. The NLRP3 gene is located on chromosome 1q44 and has 9 exons. Roughly 85% of NLRP3 mutations occur in exon 3 [29, 33]. Clinical manifestations vary among the three cryopyrinopathies, but several common features are often found, such as fever, pseudourticarial rash, joint involvement, and profoundly elevated inflammatory markers [32]. The most consistent finding across the CAPS spectrum is a migratory, maculopapular, urticaria-like, and usually nonpruritic rash. Skin biopsy reveals polymorphonuclear perivascular infiltration of the dermis, which contrasts with the biopsy findings of classical urticaria. The unique features of each of the cryopyrinopathies are described below [34].

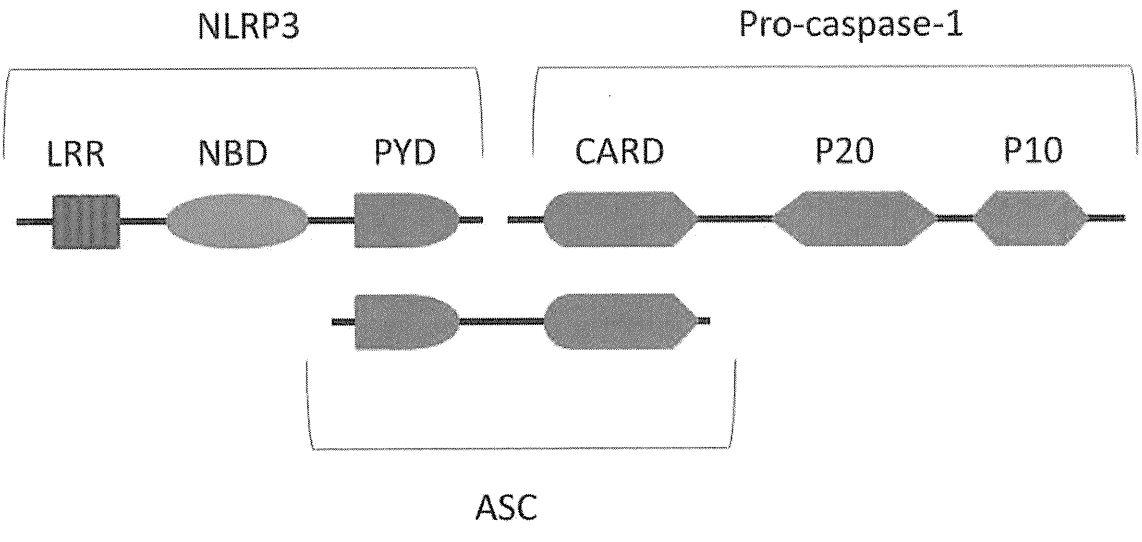

Figure 2 Schematic structure of NLRP3 inflammasome

Activation leads to the binding of NLRP3 with ACS through PYD-PYD interaction, resulting in recruiting of pro-caspase-1 via CARD-CARD interaction.

LRR: leucine-rich –repeat ; NBD:nucleotide-binding domain

PYD:pyrindomain; CARD:caspaseactivating and recruitment domain

a) Familial cold autoinflammatory syndrome (FCAS)

FCAS, also known as familial cold urticaria, is at the benign end of the CAPS spectrum, and has the most favorable prognosis of all the cryopyrinopathies [32, 35]. FCAS is characterized by episodes of low-grade fever, polyarthralgia, and nonpruritic pseudourticarial rash appearing 1-2 hours after cold exposure (range: 30 min to 6 h) and persisting for approximately 12 hours [37, 36]. Other commonly reported symptoms include conjunctivitis, profuse sweating, dizziness, headache, nausea, and extreme thirst. Symptoms are most intense in young adults, but may begin as early as childhood. Less commonly, the syndrome may present as recurrent fever, mild arthralgia, inflammatory cardiomyopathy, nephropathy, and thyroiditis, with no skin involvement. Secondary amyloidosis is

the main cause of death, occurring in up to 2% of cases [37]. Treatment includes prevention of cold exposure and, in more severe cases, anakinra. A recent study of rilonacept, a long-acting soluble receptor that binds IL-1, found good efficacy and safety in 44 patients with FCAS. NSAIDs and corticosteroids are variably effective, and antihistamines are not effective at all [38].

b) Muckle-Wells syndrome (MWS)

In 1962, Muckle & Wells described a familial syndrome of urticaria, deafness, and amyloidosis affecting nine individuals [39]. The symptoms of MWS arise in childhood, as an urticaria-like rash with low-grade fever and arthralgia. Recurring episodes of arthritis and conjunctivitis may also occur. The most characteristic manifestation of MWS is sensorineural hearing loss, which is due to chronic inflammation of the organ of Corti with cochlear nerve atrophy [40]. Less common findings include oral and genital ulcers, cystinuria, ichthyosis, recurrent abdominal pain, and microscopic hematuria. Secondary amyloidosis is common, and may occur in 1/3 to 1/4 of patients. A finding of NLRP3 mutation confirms the diagnosis. Other laboratory findings include thrombocytopenia, anemia, and increased levels of acute-phase reactants [41]. As in the other cryopyrinopathies, IL-1 receptor inhibition with anakinra can reverse the clinical manifestations of MWS, including hearing loss.

c) Neonatal onset multisystem inflammatory disease/chronic infantile neurologic, cutaneous, and articular syndrome (NOMID or CINCA syndrome)

NOMID, or CINCA syndrome, is the most severe phenotype of the cryopyrinopathy spectrum, and was first described by Prieur & Griscelli in 1981 [42]. The disease is characterized by a triad of rash, chronic aseptic meningitis, and arthropathy. Clinical manifestations arise in the first weeks of life; the cutaneous lesions often appear within hours of birth [43]. Inflammatory symptoms (such as fever) are practically continuous, with occasional flares, and affected children have severe growth retardation.

Skin lesions are found in nearly 100% of cases. CNS involvement is the second most common feature, typically presenting as chronic aseptic meningitis with leukocyte infiltration of the cerebrospinal fluid, which leads to a broad range of symptoms including chronic irritability, headaches, seizures, transient hemiplegia, and lower limb spasticity. If left untreated, approximately 80% of patients will develop sensorineural hearing loss and ocular disease, such as conjunctivitis, anterior and posterior uveitis, papilledema, and optic nerve atrophy with loss of vision [44]. Other findings include developmental delay and mental retardation. Patients with NOMID/CINCA syndrome have a typical facial appearance, characterized by frontal bossing, macrocrania, and saddle nose. The musculoskeletal changes of NOMID/CINCA syndrome can range from asymptomatic arthritis to deforming arthropathy. Most patients show inflammatory changes of the long-bone epiphyses and metaphyses, with abnormal epiphyseal calcification and cartilage overgrowth, leading to shortened limbs and joint deformities. Premature ossification of the patella, with symmetrical patellar overgrowth, is a characteristic finding [43]. The typical arthropathy of NOMID is found in 50% of patients [43].

Nonspecific laboratory changes are as in other autoinflammatory syndromes, and may include anemia, thrombocytosis, moderately increased white blood cell counts, and increased inflammatory markers, such as ESR and CRP levels. The diagnosis of NOMID/CINCA syndrome relies on adequate clinical suspicion and confirmatory genetic testing. However, only 50% of patients with a characteristic presentation of NOMID/CINCA syndrome have NLRP3 mutations, which suggests that other yet-unknown genes may also be involved in its pathophysiology.

Without early identification and treatment, the prognosis for patients with NOMID/CINCA syndrome is guarded. In addition to deforming articular involvement and neurologic sequelae, the disease carries a high risk of secondary amyloidosis in the few patients who live to adulthood. Anakinra, an IL-1 receptor antagonist, is currently the drug of choice for treatment of NOMID and has been widely used in this indication, providing significant improvement in all clinical manifestations of the disease and, consequently, patient quality of life [43]. Corticosteroids and NSAIDs can provide symptomatic relief, but have no effect on articular or neurologic involvement.

Recently, canakinumab, which targets selectively human IL-1ß with high affinity and prevents the cytokine from interaction to its receptor, is reported to effectively block the inflammatory response in CAPS. In all studies performed, canakinumab

showed a rapid improvement of symptoms of CAPS and a complete clinical response was achieved in most patients. Inflammatory markers such as C-reactive protein and serum amyloid-A protein were reduced to normal levels within few days. In comparison to other IL-1 blockers, canakinumab provides a longer plasma half-life and less injection site reactions [45, 46].

Mevalonate kinase deficiency (MKD) or hyper-IgD and periodic fever syndrome (HIDS)

HIDS follows an autosomal recessive pattern of inheritance, and is most often diagnosed in Northeastern Europe. The disease is caused by mutations in the MVK (mevalonate kinase) gene, which was discovered in 1999 [47]. MVK, which has 11 exons and is located on the long arm of chromosome 12 (locus 12q24), codes for mevalonate kinase (MK), a 396-amino acid-long enzyme. Most patients have a combination of two mutations, one of which is very often V377I. HIDS-associated mutations lead to a major reduction in MK activity (1 to 10% of normal levels), whereas mutations that completely eliminate MK function lead to a condition known as mevalonic aciduria (MA) [48, 49]. MA is a rare disease characterized by periodic fever with severe CNS involvement, mental retardation, ataxia, myopathy, poor growth, and early death.

MK plays an essential role in the isoprenoid and cholesterol synthesis pathways. It catalyzes the conversion of mevalonic acid to mevalonate 5-phosphate during the synthesis of molecules such as cholesterol, vitamin D, biliary salts, corticosteroids, and non-steroidal isoprenoid compounds. During cholesterol biosynthesis, 3-hydroxy-3-methylglutaryl-coenzyme A (HMG-CoA) reductase (the enzyme inhibited by statins) converts HMG-CoA to mevalonate, which is then phosphorylated to mevalonate phosphate. Mutations in the MVK gene block this pathway, preventing the conversion of mevalonate to mevalonate phosphate. The absence of a negative feedback loop, which is naturally provided by the presence of the end products of synthesis, leads to increased HMG-CoA reductase activity, consequently increasing serum, tissue, and urine levels of mevalonic acid. *In vitro* studies have shown that reduced synthesis of isoprenoids is associated with increased production of IL-1β [50]. Another recent in vitro study showed that MK inhibition leads to increased secretion of IL-1β due to activation of caspase-1, the enzyme that catalyzes formation of active IL-1β from its precursor [51]. High levels of immunoglobulin D (IgD) are characteristic of HIDS, but are apparently not associated with the severity of pathophysiology of the condition [52].

In MKD, febrile attacks occur more frequently in the first year of life, lasting 3 to 7 days and recurring every 4 to 6 weeks. However, the time elapsed between episodes can vary from patient to patient and even in a single individual. Febrile episodes recur for years, most frequently in childhood and adolescence, but months to years can go by between flares. Episodes may be triggered by immunization, trauma, surgery, or stress, and are characterized by high fever preceded by chills. Lymphadenopathy is extremely common. It is usually cervical, bilateral, and painful. Abdominal pain is also a frequent symptom, and may be accompanied by vomiting and/or diarrhea. Patients will also frequently report headache, and splenomegaly and hepatomegaly are common. Polyarthralgia and non-erosive arthritis of the large joints, particularly of the knees and ankles are also common. Arthritis is usually polyarticular and symmetric. Most patients have diffuse cutaneous lesions, which may consist of erythematous maculopapular rash, urticaria-like rash, erythematous nodules, petechiae, or purpura. Febrile episodes may be accompanied by sudden increase in acute phase reactant levels, including neutrophilic leukocytosis and elevated ESR, CRP, and SAA. Measurement of urinary mevalonate levels during attacks may be useful, particularly in patients with normal IgD levels.

IgD levels are persistently high (≥100 U/mL) in most patients. Nonetheless, IgD levels may be within normal limits in some HIDS patients, especially children under the age of 3 [52]. Furthermore, the finding of high IgD levels is not specific for HIDS, as it occurs in other inflammatory diseases, such as FMF and TRAPS.

The diagnosis of MKD is confirmed by a finding of MVK mutations. However, the presence of a clinical phenotype consistent with the disease in conjunction with high serum IgD and urinary mevalonate levels may suggest the diagnosis.

Most of the usual treatments, such as NSAIDs, corticosteroids, IVIG, colchicine, and thalidomide, are ineffective in HIDS. The involvement of MK in the cholesterol synthesis pathway has encouraged the introduction of statins in the management of MKD; the efficacy of simvastatin, an HMG-CoA reductase inhibitor, has been demonstrated in 5/6 of MKD pa-

tients [53]. Use of etanercept and anakinra in refractory cases has also been reported [54, 55, 56]. Recently two patients with MVA have been treated successfully with stem cell transplantation [57].

Pyogenic aseptic arthritis, pyoderma gangrenosum, and acne syndrome (PAPA syndrome)

PAPA syndrome is an autosomal dominant disease characterized by sterile, deforming arthritis, skin ulcers (pyoderma gangrenosum), and severe cystic acne. Unlike other autoinflammatory syndromes, PAPA does not have fever as its most prominent symptom.

PAPA syndrome is caused by mutations in the gene that codes proline-serine-threonine phosphatase interacting protein 1 (PSTPIP1), and only five associated mutations have been reported thus far. PSTPIP1 is a 416-amino acid-long protein expressed mostly in neutrophils. Mutations in PSTPIP1 are believed to lead to hyperphosphorylation of the protein, which could increase the potency of its binding to pyrin, with subsequent activation of IL-1β production, as seen in FMF [58].

Deficiency of interleukin-1–receptor antagonist (DIRA)

A new autosomal recessive AIS, caused by mutations in the IL1RN gene, which codes for interleukin-1 receptor antagonist (IL1Ra), was reported recently [59]. The syndrome, which was described in 10 patients, was given the name "deficiency of interleukin-1 receptor antagonist" (DIRA) and is characterized by early onset of symptoms, most frequently in the neonatal period.

Patients with DIRA present with pustulosis, multifocal aseptic osteomyelitis, and markedly elevated ESR and CRP levels. Skin involvement may range from sparse pustules to generalized pustular dermatitis or ichthyosiform lesions. Skin biopsy may reveal neutrophilic infiltration of the epidermis and dermis, pustules in the stratum corneum, acanthosis, and hyperkeratosis. All patients described in the report had osteomyelitis, characterized by pain with movement and periarticular swelling; the most frequent radiological findings were widening of the costal arches, periosteal elevation along long bones, and multifocal osteolytic lesions.

As in the other pyogenic autoinflammatory syndromes (PAPA and Majeed syndrome), fever is not a striking feature of DIRA, and was not present in any of the patients described. Two of the 10 patients had interstitial lung disease, and three died before therapy could be attempted (at 2 months, 21 months, and 9 years of age respectively).

The treatment of choice is recombinant IL-1RA (anakinra), which produces a dramatic response in skin and bone symptoms and in the quality of life of patients with DIRA.

Pitfall for diagnosis of NOMID/CINCA syndrome

Recent genetic studies revealed that CAPS patients usually carry heterozygous mutations in the NLRP3 coding region (mutation positive patients) [60, 61, 62, 63, 64, 65]. Although they exhibit no recognizable differences in clinical symptoms or in their response to treatment, approximately half of CINCA syndrome patients lack detectable mutations in NLRP3, as assessed by conventional genomic sequencing (mutation-negative patients) [32, 60, 61, 62, 66, 67], indicating the existence of genetic heterogeneity among CAPS patients. Recently, we reported a patient with CINCA syndrome exhibiting mosaicism of a disease-associated mutation of NLRP3 [68]. This case suggested that some mutation-negative CAPS patients might have mosaicism of the NLRP3 mutation; however, the contribution of NLRP3 mosaicism to disease is controversial. Aksentijevich et al claimed that NLRP3 mosaicism is a rare event in mutation-negative patients, based on their analysis of 14 patients in which NLRP3 mosaicism was not identified, even with careful bidirectional sequencing [32, 68].

Somatic mosaicism has been reported in a number of autosomal dominant monogenic diseases [69]. Diagnosis of mosaicism by conventional genomic sequencing using the dideoxy termination method is often difficult, because the overlapping chromatogram of the mutant is easily missed when the frequency of a mutant allele is less than 20% to 30%. Heteroduplex-based methods or subcloning-based analysis of mutant alleles enable one to detect such low-level mosaicism; however, these methods are resource intensive, and cannot distinguish whether the detected mutation is disease-causing or simply a nonfunctional single nucleotide polymorphism (SNP). An alternative approach involves the isolation of mutant cells using functional analyses based on their characteristic biologic features, and then determining the DNA sequence of the isolated cells. Based on these backgrounds, we set out to identify specific biologic features of NLRP3-mutant cells compared

with nonmutated cells, in an effort to specifically isolate NLRP3-mutated cells from mutation-negative patients [70].

Disease-associated NLRP3 mutations induce ASC-dependent NF-κB activation in some systems, and we reported that they also induce necrotic cell death in the human monocytic cell line THP-1, which is a novel function of NLRP3 [68]. Based on these backgrounds, we explored whether NLRP3-mutant cells have specific biologic features, using monocytes from mutation-positive patients, and found that NLRP3-mutant monocytes rapidly underwent necrosis-like cell death after treatment with lipopolysaccharide (LPS) to induce NLRP3 expression. This unique phenotype of NLRP3 mutant cells enabled us to differentiate NLRP3-mutated cells and nonmutated cells in 3 of 4 mutation-negative CAPS patients, and we were able to successfully demonstrate that these 3 patients had mutations of NLRP3 as latent mosaicism (Fig. 3) [71, 72].

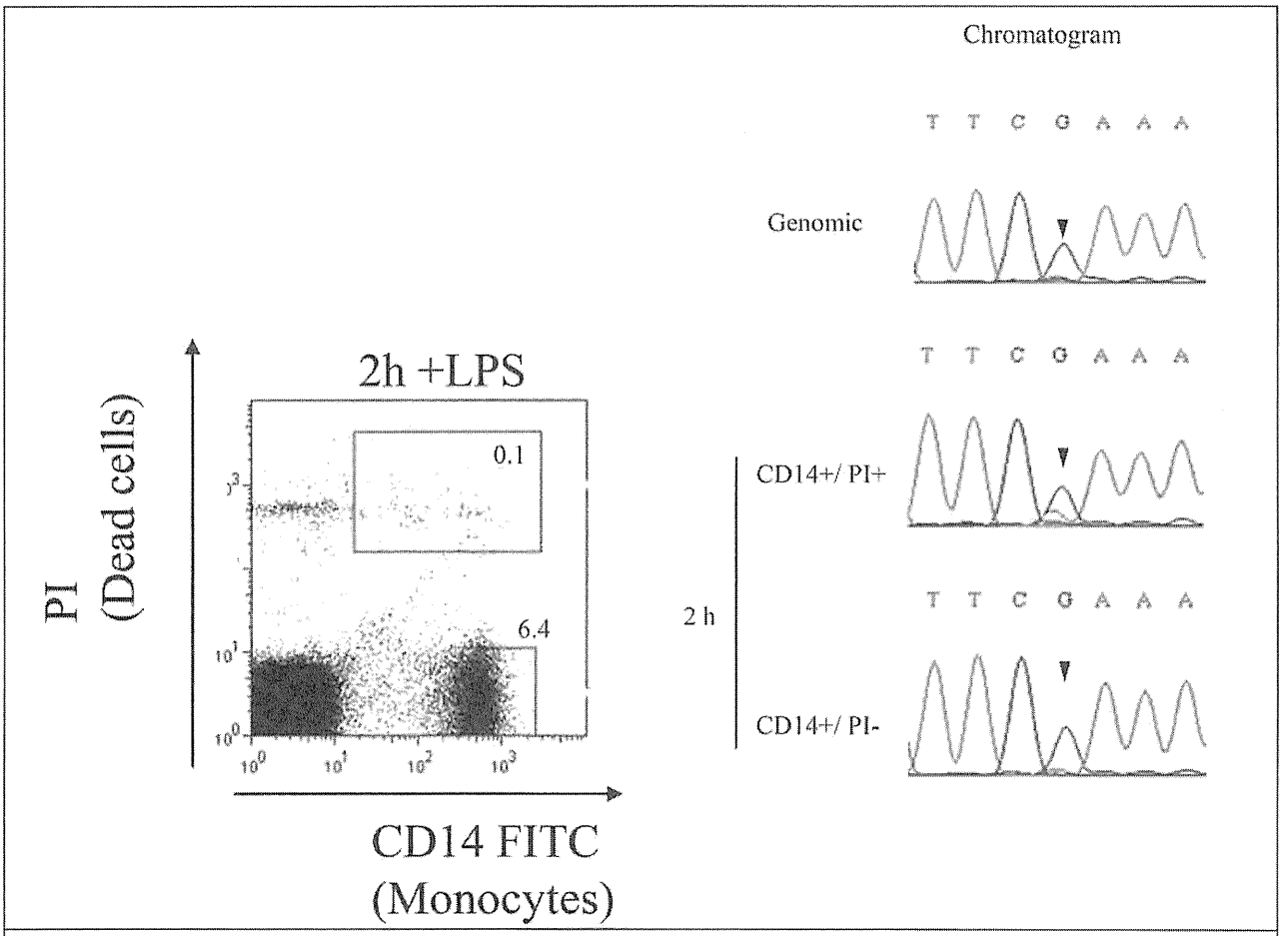

Fig. 3 Enrichment of dying monocytesin mutation-negative patient revealed latent overlapping peaks

PBMCs from mutation-negative CAPS patient were cultured with or without LPS (10 ng/mL) for 24 hours. CD14-positive and -negative cells were sorted, and DNA was extracted and sequenced for analysis of NLRP3.

Reference

1) Medzhitov R: new adventures of an old flame. Cell Inflammation. 2010; 140: 771-776.

2) FranchiL, Warner N, Viani K, Nunez G: Function of Nod-like receptors in microbial recognition and host defense. Immunol Rev. 2009; 227: 106-128.

3) Martinon F, Mayor A, Tschopp J: The inflammasomes: guardians of the body. Annu Rev. Immunol. 2009; 27: 229-265.

4) Mitroulis I, Skendros P, Ritis K: Targeting IL-1β in disease; the expanding role of NLRP3 inflammasome. Eur J Inter Med. 2010; 21: 157-163.

5) Masters LS, Simon A, Aksentijevich I, Kastner DL. Horror antoinflammaticus: the molecular pathphysiology of autoinflammatory disease. Annu Rev.

Immunol. 2009; 27: 621-628.

6) Kastner DL, Aksentijevich I, Goldbach-Mansky R. Autoinflammatory disease reloated: a clinical perspective. Cell. 2010; 140: 784-790.

7) Chen M, Wang H, Chen W, Meng G: Regulation of adaptive immunity by the NLRP3 inflammasome. Int Immunopharmacol. 2010; Nov 27. [Epub ahead of print]

8) Hornung V, Latz E: Intracellular recognition. Nat Rev. Immunol. 2010; 10: 123-130.

9) Unterholzner L, Keating SE, Baran M, Horan KA, Jensen SB, Sharma S, Sirois CM, Jin T, Latz E, Xiao TS, Fitzgerald KA, Paludan SR, Bowie AG: FI16 is an innate immune sensor for intracellular DNA. Nat Immunol. 2010; 11: 997-1004.

10) Iwasaki A, Medzhitov R: Regulation of adaptive immunity by the innate immune system. Science. 2010; 327: 291-295.

11) Takeuchi O, Akira S: Pattern recognition receptors and inflammation. Cell. 2010; 140: 805-820.

12) Franchi L, Eigenbrod T, Munoz-Planillo R, Nunez G: The inflammasome: a caspase- 1-activation platform that regulates immune responses and disease pathogenesis. Nat. Immunol. 2009; 10: 241-247.

13) Martinon F, Burns K, Tschopp J. The inflammasome: a molecular platform triggering activation of inflammatory caspases and processing of pro-IL-beta. Mol Cell. 2002; 10: 417-426.

14) Schroder K, Tschopp J: The inflammasomes. Cell. 2010; 140: 821-832.

15) Anderson JP, Mueller JL, Rosengren S, Boyle DL, Schaner P, Cannon SB, Goodyear CS, Hoffman HM: Structural, expression, and evolutionary analysis of mouse CIAS1. Gene. 2004; 338: 25-34.

16) Sutterwala FS, Ogura Y, Szczepanik M, Lara-Tejero M, Lichtenberger GS, Grant EP, Bertin J, Coyle AJ, Galán JE, Askenase PW, Flavell RA: Critical role for NALP3/CIAS1/Cryopyrin in innate and adaptive immunity through its regulation of caspase-1. Immunity. 2006; 24: 317-327.

17) Bauernfeind FG, Horvath G, Stutz A, Alnemri ES, MacDonald K, Speert D, Fernandes-Alnemri T, Wu J, Monks BG, Fitzgerald KA, Hornung V, Latz E. Cutting edge: NF-kappaB activating pattern recognition and cytokine receptors license NLRP3 inflammasome activation by regulating NLRP3 expression. J Immunol. 2009; 183: 787-791.

18) McCall SH, Sahraei M, Young AB, Worley CS, Duncan JA, Ting JP, Marriott I: Osteoblasts express NLRP3, a nucleotide-binding domain and leucine-rich repeat region containing receptor implicated in bacterially induced cell death. J Bone Miner Res. 2008; 23: 30-40.

19) Gattorno M, Tassi S, Carta S, Delfino L, Ferlito F, Pelagatti MA, D'Osualdo A, Buoncompagni A, Alpigiani MG, Alessio M, Martini A, Rubartelli A: Pattern of interleukin-1beta secretion in response to lipopolysaccharide and ATP before and after interleukin-1 blockade in patients with CIAS1 mutations. Arthritis Rheum. 2007; 56: 3138-3148.

20) Nakamura Y, Kambe N, Saito M, Nishikomori R, Kim YG, Murakami M, Núñez G, Matsue H: Mast cells mediate neutrophil recruitment and vascular leakage through the NLRP3 inflammasome in histamine-independent urticaria. J Exp Med. 2009; 206: 1037-1046.

21) Kummer JA, Broekhuizen R, Everett H, Agostini L, Kuijk L, Martinon F, van Bruggen R, Tschopp J: Inflammasome components NALP 1 and 3 show distinct but separate expression profiles in human tissues suggesting a site-specific role in the inflammatory response. J Histochem Cytochem. 2007; 55: 443-452.

22) Ogura Y, Sutterwala FS, Flavell RA. The inflammasome: first line of the immune response to cell stress. Cell. 2006; 126: 659-662.

23) Allen IC, Scull MA, Moore CB, Holl EK, McElvania-TeKippe E, Taxman DJ, Guthrie EH, Pickles RJ, Ting JP: The NLRP3 inflammasome mediates in vivo innate immunity to influenza A virus through recognition of viral RNA. Immunity. 2009; 30: 556-565.

24) Meng G, Strober W: New insights into the nature of autoinflammatory diseases from mice with Nlrp3 mutations. Eur J Immunol. 2010; 40: 649-653.

25) Chung Y, Chang SH, Martinez GJ, Yang XO, Nurieva R, Kang HS, Ma L, Watowich SS, Jetten AM, Tian Q, Dong C: Critical regulation of early Th17 cell differentiation by interleukin-1 signaling. Immunity. 2009; 30: 576-587.

26) Meng G, Zhang F, Fuss I, Kitani A, StroberW: A mutation in the Nlrp3 gene causing inflammasome

hyperactivation potentiates Th17 cell-dominant immune responses. Immunity. 2009; 30: 860-874.

27) Eisenbarth SC, Colegio OR, O'Connor W, Sutterwala FS, Flavell RA: Crucial role for the Nalp3 inflammasome in the immunostimulatory properties of aluminium adjuvants. Nature. 2008; 453: 1122-1126.

28) Spreafico R, Ricciardi-Castagnoli P, Mortellaro A: The controversial relationship between NLRP3, alum, danger signals and the next-generation adjuvants. Eur J Immunol. 2010; 40: 638-642.

29) Hoffman HM, Mueller JL, Broide DH, Wanderer AA, Kolodner RD: Mutation of a new gene encoding a putative pyrin-like protein causes familial cold autoinflammatory syndrome and Muckle–Wells syndrome. Nat Genet. 2001; 29: 301-305.

30) Ting JPY, Kastner DL, Hoffman HM: CATERPILLERs, pyrin and hereditary immunological disorders. Nat Rev Immunol. 2006; 6: 183-195.

31) Aksentijevich I, Nowak M, Mallah M, Chae JJ, Watford WT, Hofmann SR, Stein L, Russo R, Goldsmith D, Dent P, Rosenberg HF, Austin F, Remmers EF, Balow JE Jr, Rosenzweig S, Komarow H, Shoham NG, Wood G, Jones J, Mangra N, Carrero H, Adams BS, Moore TL, Schikler K, Hoffman H, Lovell DJ, Lipnick R, Barron K, O'Shea JJ, Kastner DL, Goldbach-Mansky R: De novo CIAS1 mutations, cytokine activation, and evidence for genetic heterogeneity in patients with neonatal-onset multisystem inflammatory disease (NOMID): a new member of the expanding family of pyrin-associated autoinflammatory diseases. Arthritis Rheum. 2002; 46: 3340-3348.

32) Aksentijevich I, D Putnam C, Remmers EF, Mueller JL, Le J, Kolodner RD, Moak Z, Chuang M, Austin F, Goldbach-Mansky R, Hoffman HM, Kastner DL: The clinical continuum of cryopyrinopathies: novel CIAS1 mutations in North American patients and a new cryopyrin model. Arthritis Rheum. 2007; 56: 1273-1285.

33) Aróstegui JI, Aldea A, Modesto C, Rua MJ, Argüelles F, González-Enseñat MA, Ramos E, Rius J, Plaza S, Vives J, Yagüe J: Clinical and genetic heterogeneity among Spanish patients with recurrent autoinflammatory syndromes associated with the CIAS1/PYPAF1/NALP3 gene. Arthritis Rheum. 2004; 50: 4045-4050

34) Jesus AA, Oliveira JB, Hilário MO, Terreri MT, Fujihira E, Watase M, Carneiro-Sampaio M, Silva CA: Pediatric hereditary autoinflammatory syndromes. J Pediatr (Rio J). 2010: 86; 353-366.

35) Jesus AA, Silva CA, Segundo GR, Aksentijevich I, Fujihira E, Watanabe M, Carneiro-Sampaio M, Duarte AJ, Oliveira JB. Phenotype-genotype analysis of cryopyrin-associated periodic syndromes (CAPS): description of a rare non-exon 3 and a novel CIAS1 missense mutation. J Clin Immunol. 2008; 28: 134-138.

36) Hoffman HM, Wanderer AA, Broide DH. Familial cold autoinflammatory syndrome: phenotype and genotype of an autosomal dominant periodic fever. J Allergy Clin Immunol. 2001; 108: 615-620.

37) Rigante D: Autoinflammatory syndromes behind the scenes of recurrent fevers in children. Med Sci Monit. 2009; 15: RA179-187.

38) Gandhi C, Healy C, Wanderer AA, Hoffman HM. Familial atypical cold urticaria: description of a new hereditary disease. J Allergy Clin Immunol. 2009; 124: 1245-1250.

39) Muckle TJ, Wells. Urticaria, deafness, and amyloidosis: a new heredo-familial syndrome. Q J Med. 1962; 31: 235-248.

40) Dodé C, Le Dû N, Cuisset L, Letourneur F, Berthelot JM, Vaudour G, Meyrier A, Watts RA, Scott DG, Nicholls A, Granel B, Frances C, Garcier F, Edery P, Boulinguez S, Domergues JP, Delpech M, Grateau G: New mutations of CIAS1 that are responsible for Muckle-Wells syndrome and familial cold urticaria: a novel mutation underlies both syndromes. Am J Hum Genet. 2002; 70: 1498-1506.

41) Hawkins PN, Lachmann HJ, Aganna E, McDermott MF: Spectrum of clinical features in Muckle-Wells syndrome and response to anakinra. Arthritis Rheum. 2004; 50: 607-612.

42) Prieur AM, Griscelli C: Arthropathy with rash, chronic meningitis, eye lesions, and mental retardation. J Pediatr. 1981; 99: 79-83.

43) Goldbach-Mansky R, Dailey NJ, Canna SW, Gelabert A, Jones J, Rubin BI, Kim HJ, Brewer C, Zalewski C, Wiggs E, Hill S, Turner ML, Karp BI, Aksentijevich I, Pucino F, Penzak SR, Haverkamp MH, Stein L, Adams BS, Moore TL, Fuhlbrigge RC, Shaham B, Jarvis JN, O'Neil K, Vehe RK, Beitz LO, Gardner G, Hannan WP, Warren RW, Horn W, Cole